

NOTCHED BUSBAR DESIGN GUIDELINES FOR CORELESS ACS37610 DIFFERENTIAL CURRENT SENSOR

By Yannick Vuillermet
Allegro MicroSystems

INTRODUCTION

The ACS37610 is a Hall plate-based differential current sensor designed to measure current flowing in a busbar or a PCB, without using a ferromagnetic concentrator core. The ACS37610 is well-suited for electric vehicle applications (all-electric, hybrid, or plug-in), such as inverters, charging stations, on-board chargers, or DC links. This application note focuses on how a busbar should be designed to achieve optimum performance with this sensor.

The ACS37610 is a contactless current sensor and features differential sensing to reject common-mode stray magnetic fields. It is recommended for typical current measurement ranging from 200 A to more than 2000 A. Due to its low noise Hall plates, a good resolution can be achieved without the use of a ferromagnetic concentrator core. When higher accuracy is required, Allegro recommends the use of a ferromagnetic concentrator core in conjunction with A1365, A1367, or ACS70310 linear ICs.

While the ACS37610 would function using any busbar design, to achieve the greatest performance (accuracy, high signal-to-noise ratio, high bandwidth, low sensitivity to mechanical tolerances, etc.), the busbar must include certain features. As shown in Figure 1, the ACS37610 is placed over a notch (or neckdown) in the busbar. This notch is intended to locally increase the current density and the signal measured by the IC. Note that in Figure 1, the ACS37610 is placed on top of the PCB. To reduce the distance between the Hall plates and the busbar, the ACS37610 could also be placed on the other side of the PCB. In this case, high-voltage isolation requirements should be considered.

Figure 2 illustrates how the ACS37610 senses the magnetic field induced by the current I flowing in the busbar. The ACS37610 has two Hall plates, sensitive along the Z axis

and 2.58 mm away from each other. The left Hall plate measures the magnetic field B_L , and the right Hall plate measures the magnetic field B_R . The output of the sensor, V_{OUT} , is proportional to the differential magnetic field, ΔB (equation 1 and equation 2). α is the ACS37610 output sensitivity to magnetic field. The relationship between the applied current and the differential field is given by the coupling factor, CF (equation 3). The equation 4 indicates the relationship between the IC sensitivity α , the coupling factor CF , the IC output range ΔV and the total current range $\Delta I = I_{max} - I_{min}$. The definition of the current resolution or RMS output noise δ is given in equation 5, where ϵ is the input referred noise density (0.8 mGrms/ $\sqrt{\text{Hz}}$ typical for ACS37610 at room temperature), and BW is the application required bandwidth. To achieve the highest resolution, the coupling factor should be the highest.

$$\Delta B = B_R - B_L \quad (1)$$

$$V_{OUT} = \alpha \times \Delta B \quad (2)$$

$$\Delta B = CF \times I \quad (3)$$

$$\alpha = \Delta V / (\Delta I \times CF) \quad (4)$$

$$\delta = \frac{\epsilon \times \sqrt{BW \times \pi / 2}}{CF} \quad (5)$$

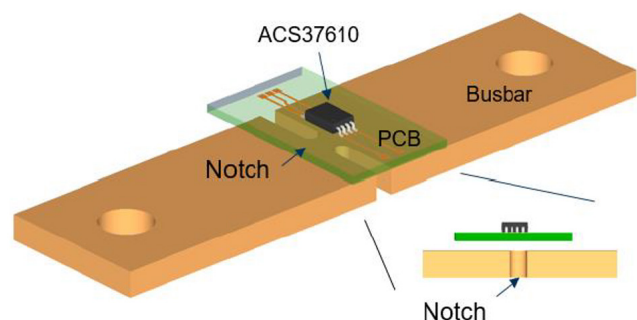


Figure 1: System overview

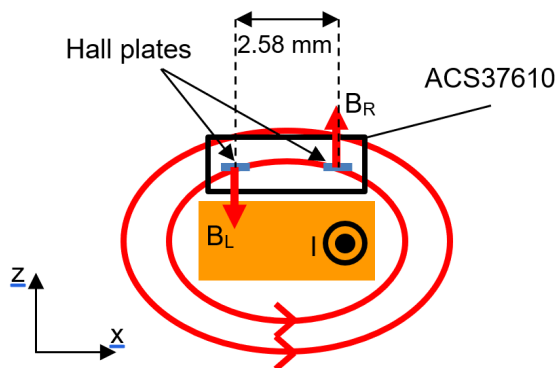


Figure 2. ACS37610 measurement principle

Table 1 indicates all available versions of ACS37610. The ACS37610 has a wide range of programming sensitivities: from 2.5 to 30 mV/G. Hence, it covers a wide range of measurable current: from a few hundreds to a few thousands (Figure 3 is an example assuming a 5 V IC, a bipolar output having 4 V range, and $\Delta I = 2 \times I_{peak}$).

The ACS37610 sensitivity is customer programmable. This feature is especially useful to improve the measurement accuracy by calibrating out the mechanical mounting tolerances. Indeed, the sensitivity can be reprogrammed once the ACS37610 is mounted in the application.

Table 1

Part Number	Sensitivity Typical α [mV/G]	Output Range ΔV [V]	Sensitivity Trim Range [mV/G]
20B5	20	4.0	10 to 30
20U5	20	2.7	10 to 30
10B5	10	4.0	5 to 20
5B5	5	4.0	2.5 to 7.5
10b3	10	4.0	5 to 20

This application note provides guidelines on how the notch should be designed to achieve optimal performances using the ACS37610. Indeed, the notch design results in a compromise between a high signal-to-noise ratio (equivalent to a high coupling factor), low additional electrical resistance, and some good AC/transient performances (if required).

This application note also provides, in the appendices, some lookup tables to cover the expected AC and DC performances of various notch dimensions.

Note that all results in this document come from 3D FEM electromagnetic simulations.

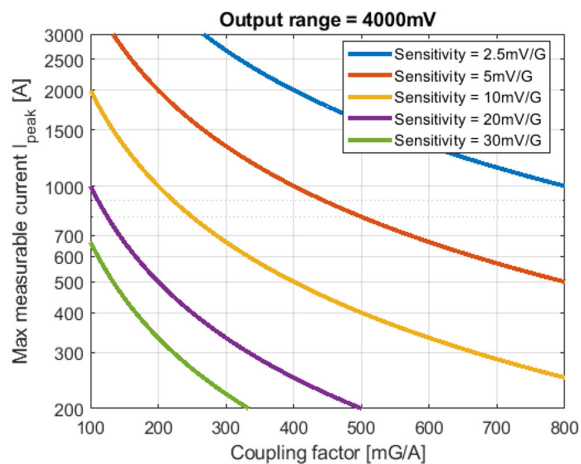


Figure 3: Max measurable current versus Coupling Factor versus selected Sensitivity

Busbar Design: Definitions

The busbar parameters (Figure 4) are the busbar thickness T , the busbar width W , the notch width N , the notch length L , and the air gap AG from the top of the busbar to the Hall plates (Figure 5).

The busbar thickness T and width W are often fixed to meet the application maximum current. Most of the time, the air gap is also fixed by the mechanical and voltage isolation constraints. Therefore, the notch dimensions L and N are usually considered to adapt the coupling factor to the application specifications. In this document, the edges of the notch have a 1 mm radius fillet. The minimum width N is limited by the mechanical robustness of a narrow notch and the additional electrical resistance it induces, which leads to additional heat to be dissipated.

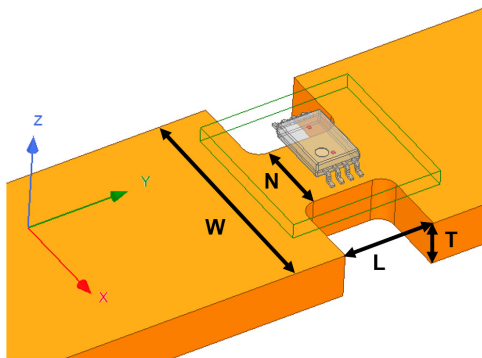


Figure 4: Busbar and notch parameters description

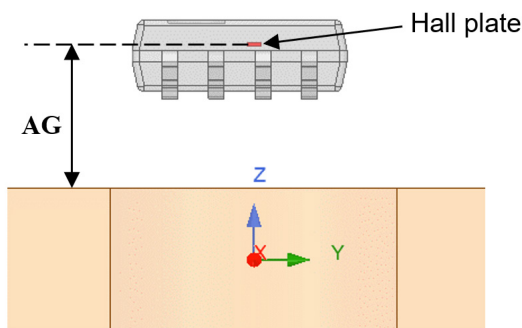


Figure 5: Air gap definition

Coupling Factor versus Notch Dimensions

In this section, the coupling factor and the achievable resolution will be given for various dimensions of the busbar and notch, while assuming a DC input current.

From a previous application note (“Guidelines for designing a busbar with notch for Allegro’s coreless ACS37612 differential current sensor”), it appears that the coupling factor does not depend significantly on the notch length L and the busbar width W . In the following, the busbar width is fixed to $W = 15$ mm as it is a typical busbar width. Nevertheless, the results in this document are valid for whatever width $W \geq 10$ mm. The default value selected for the notch length is $L = 6$ mm as it is a good compromise between DC performances, AC performances (see later section “Behavior Over Frequency”) and additional resistance. Some results with $L = 3$ mm are available in the appendices, at the end of this document (Figure 14).

Figure 6 shows the mapping of coupling factors versus air gap AG and notch width N for various busbar thicknesses T . One can see that the coupling factor highly depends on the notch width and on the air gap: highest coupling factors are associated with smallest notch widths and smallest air gaps. As said before, the air gap and the busbar thickness usually cannot be modified easily. Thus, the notch width N is the primary parameter that is used to achieve the required coupling factor.

Figure 7 displays the corresponding current resolution with a 50 kHz measurement bandwidth. This bandwidth corresponds to typical automotive inverter applications: it guarantees flat output behavior up to few kHz. The current resolution is in the range of 0.5 to 1.5 A_{rms} . The same figure (Figure 15) is given with a 10 kHz measurement bandwidth in the appendices, corresponding to typical DC applications.

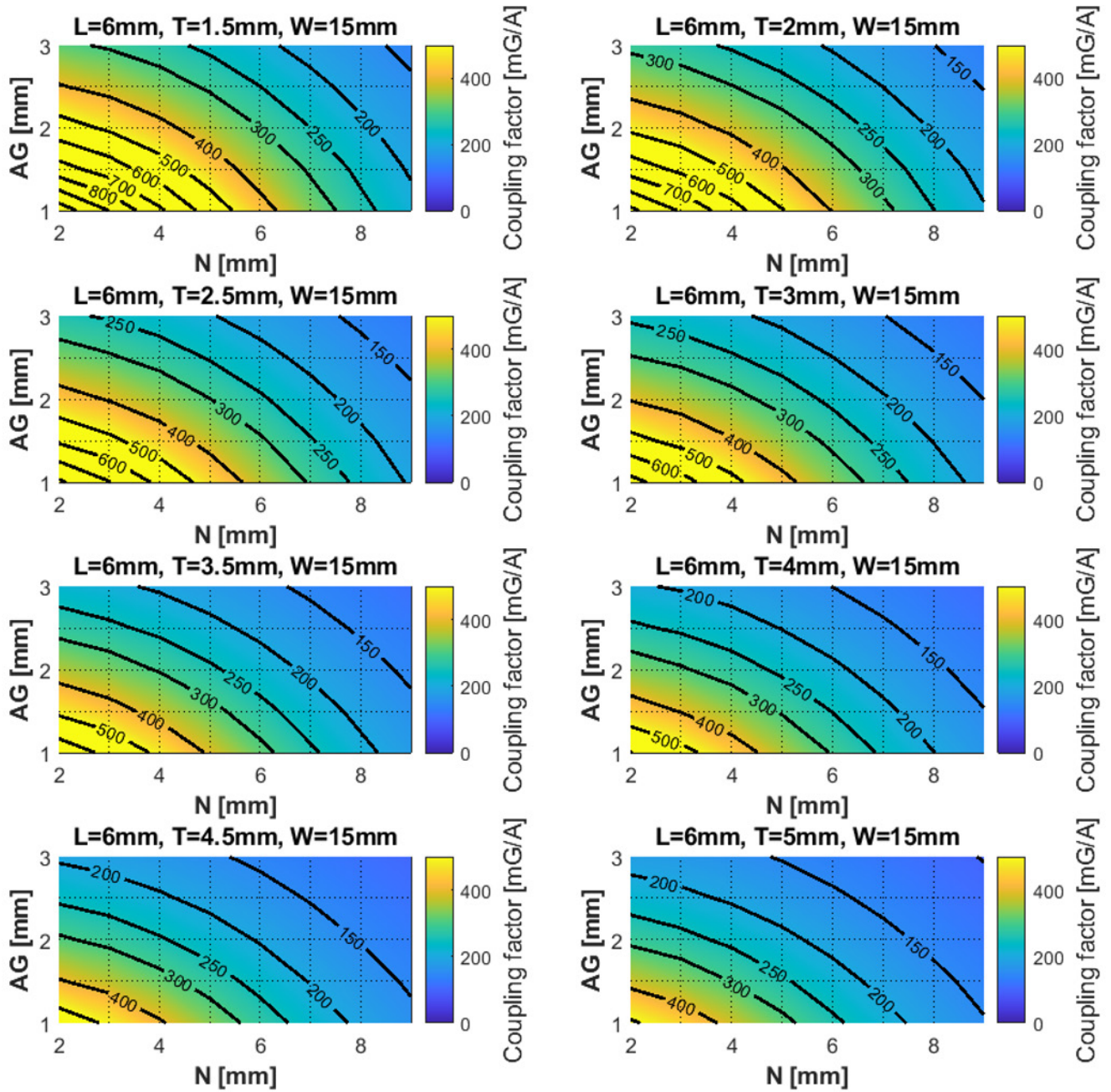


Figure 6: Coupling factor versus AG and N for various busbar thicknesses (L = 6 mm, W = 15 mm)

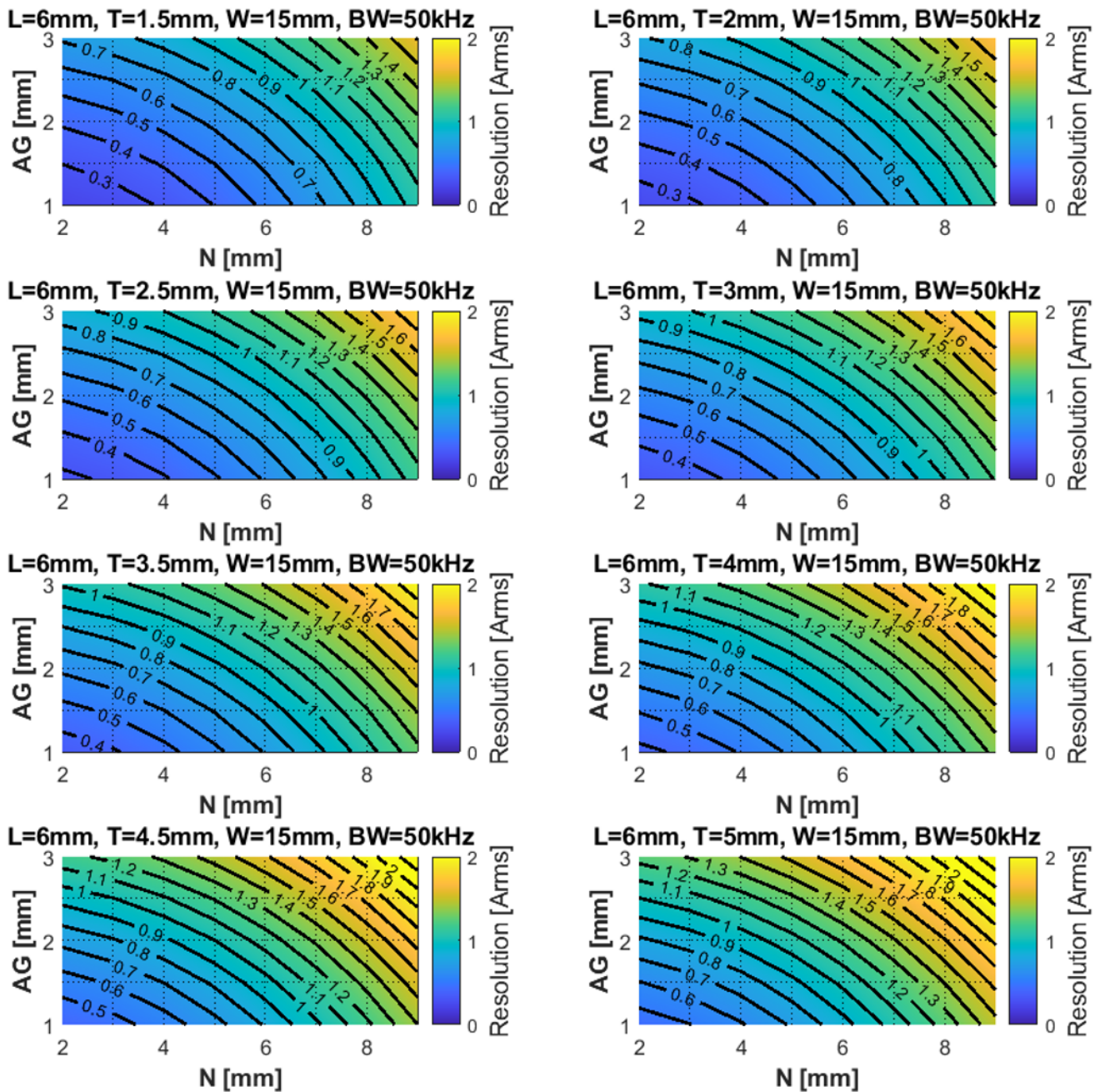


Figure 7: Resolution versus AG and N for various busbar thicknesses, at 50 kHz (L = 6 mm, W = 15 mm)

Behavior Over Frequency

All results discussed so far were assuming a continuous DC current flowing in the conductor. When an AC current is driven in the busbar, eddy currents are generated in this busbar. They tend to modify the current distribution inside the conductor: from a uniform density at low frequency, the density becomes higher near the surface of the conductor at high frequency (Figure 8).

These variations of the current density modify the magnetic field distribution around the notch. Therefore, the differential magnetic field measured by the ACS37610 in AC is altered compared to the magnetic field measured with a DC current. It implies a variation of the coupling factor (Figure 9) and a phase delay (Figure 10) in the measurements. These two latest figures are given for $T = 3$ mm and $L = 6$ mm. The thicknesses $T = 1$ mm, $T = 2$ mm, and $T = 4$ mm are available in the appendices, as well as results with $L = 3$ mm (Figure 16 to Figure 29).

The coupling factor variations due to AC current are relatively small over air gap but large versus notch width N and current frequency. From a design point of view, it is recommended to use a notch as narrow as possible to reduce eddy current effect. Indeed, with a smaller notch, there is less room for the eddy current to significantly modify a uniform current density. A long notch L is also

recommended to reduce the eddy current: in this case, the IC measurement is not affected by the large eddy current induced outside the notch.

It should be noted that the bandwidth of the current measurement is, most of the time, not limited by the ACS37610 bandwidth (250 kHz) but instead by the eddy current in the busbar.

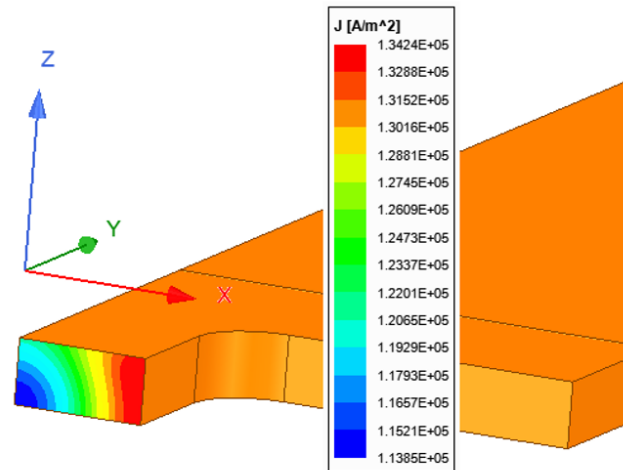


Figure 8: Current density inside the notch at 2 kHz ($L = 6$ mm, $N = 4$ mm, $T = 2$ mm, $W = 15$ mm, $I = 1$ A). Only a portion of the busbar is shown due to symmetries.

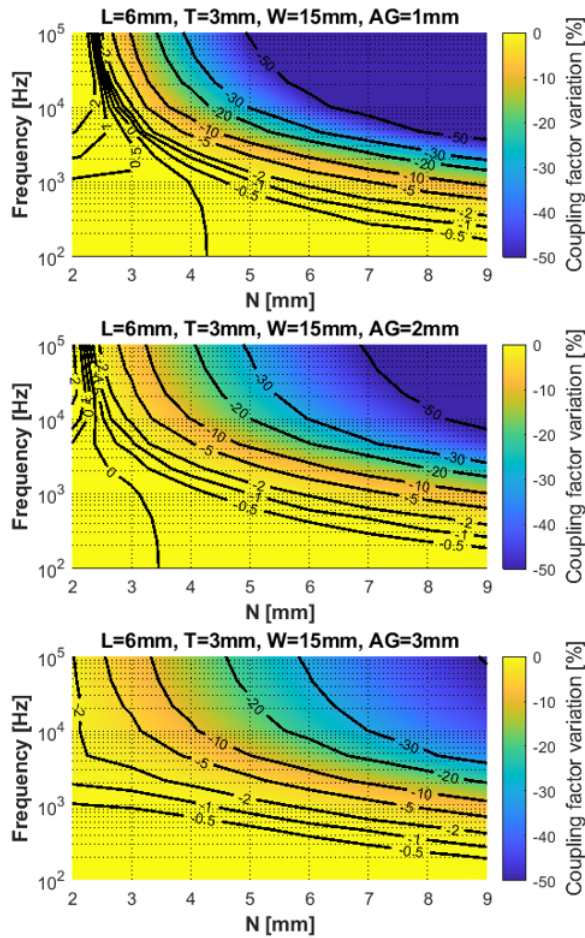


Figure 9: Coupling factor loss over frequency and air gap, due to eddy current in the busbar ($L = 6 \text{ mm}$, $T = 3 \text{ mm}$, $W = 15 \text{ mm}$)

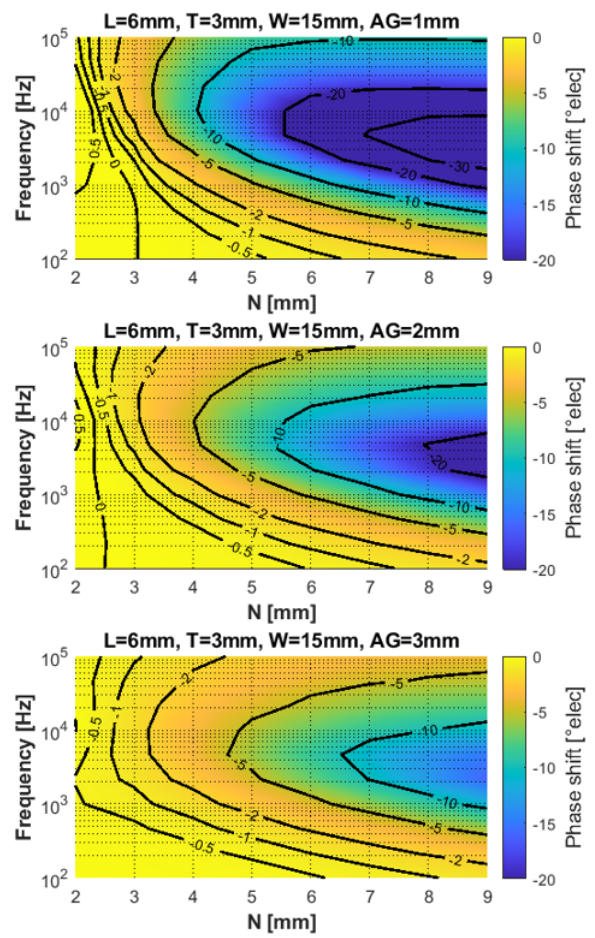


Figure 10: Phase delay over frequency and air gap, due to eddy current in the busbar ($L = 6 \text{ mm}$, $T = 3 \text{ mm}$, $W = 15 \text{ mm}$)

Thermal Considerations

This document does not focus on thermal considerations, but they must be kept in mind when designing the busbar. The thermal behavior of the complete system highly depends on the surrounding environment (heat source nearby, proximity of other materials, etc.), the cooling system (active or passive) if any, on-time duration, and the current density flowing in the busbar. The typical current densities used in automotive inverter applications are in the range of 10 to 30 A/mm².

Figure 11 indicates the resistance increase ΔR_r of the busbar total resistance due to the added notch, for a busbar thickness $T = 1$ mm and width $W = 15$ mm. These resistances come from DC conduction FEM simulations.

For some different values of T and W , the following equation gives an estimation of the additional resistance:

$$\Delta R(T, W) = \frac{1}{T} \times \left(\Delta R_r + \frac{L}{\sigma} \times \left(\frac{1}{15.10^{-3}} - \frac{1}{W} \right) \right) \quad (6)$$

Where σ is the copper conductivity ($\sigma = 58e6S/m$) and L the notch length.

For example, adding a notch with $N = 4.5$ mm and $L = 6$ mm to a $W = 17$ mm and $T = 3$ mm busbar will increase the total busbar resistance by $8.5 \mu\Omega$ ($= 24 / 3 + 6 / 3 / 58 \times (1 / 15.10^{-3} - 1 / 17.10^{-3})$). For a 1000 A peak sinusoidal current, this is equivalent to $4.25 W$ ($= 8.5e-6 \times (1000/\sqrt{2})^2$) additional heat.

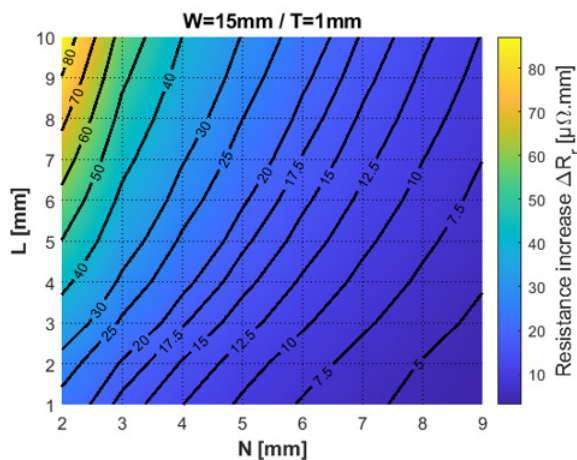


Figure 11: Busbar resistance increase due to the notch, with $T = 1$ mm and $W = 15$ mm

Sensitivity to Mechanical Tolerances

The coupling factor between the busbar and the ACS37610 is modified when the IC is not perfectly placed above the neckdown. A modification of the coupling factor directly translates into a sensitivity variation of the IC output (from equations 2 and 3).

It is recommended to reprogram the sensitivity in the application once mounted in order to compensate for mounting placement error. After mounting, the coupling factor would only vary due to vibrations, thermal expansion and/or lifetime displacement of the IC with respect to the busbar.

Left plots of Figure 12 report the coupling factor variations due to misplacement along x , y , and z axis, given for $L = 6$ mm, $T = 3$ mm, and $W = 15$ mm. The variations are given in percentage of the nominal placement coupling factor and for a $100 \mu m$ misplacement. For example, assuming ± 0.5 mm placement accuracy in all three directions, a busbar with $L = 6$ mm, $T = 3$ mm, $W = 15$ mm, $AG = 2$ mm, and $N = 4$ mm would see coupling factor variations of -3.0% ($\approx -0.6 \times 5$, where $-0.6\%/100 \mu m$ comes from the Figure 12 at $AG = 2$ mm and $N = 4$ mm and 5 is $5 \times 100 \mu m = 0.5$ mm) along x , $+0.0\%$ along y , and -20.0% ($\approx -4.0 \times 5$) along z .

The misplacement along z , i.e. air gap, appears to be the most critical tolerance, especially with thin width (small N). The air gap variations must be well-controlled in the application with respect to vibrations, thermal expansion, and lifetime displacement to use the ACS37610 in an optimal manner.

From a general point of view, the sensitivity tolerance to misplacements is smaller with larger neckdown.

Right plots of Figure 12 report the coupling factor variations due to an IC tilt around x , y , and z axis, given for a $L = 6$ mm, $T = 3$ mm, and $W = 15$ mm. The variations are given in percentage of the nominal coupling factor and for a 1° tilt. These plots demonstrate that the coupling factor is sensitive to IC tilts but does not depend much on air gap and notch width. The most critical tilt is around y axis.

For example, assuming $\pm 3^\circ$ tilt in all three directions, the previous notch would see coupling factor variations of -0.3% ($\approx -0.1 \times 3$, where $-0.1\%/^\circ$ is the rounding of the look-up table value of $-0.076\%/^\circ$) around x , -0.6% ($\approx -0.2 \times 3$) around y , and -0.3% ($\approx -0.1 \times 3$) around z .

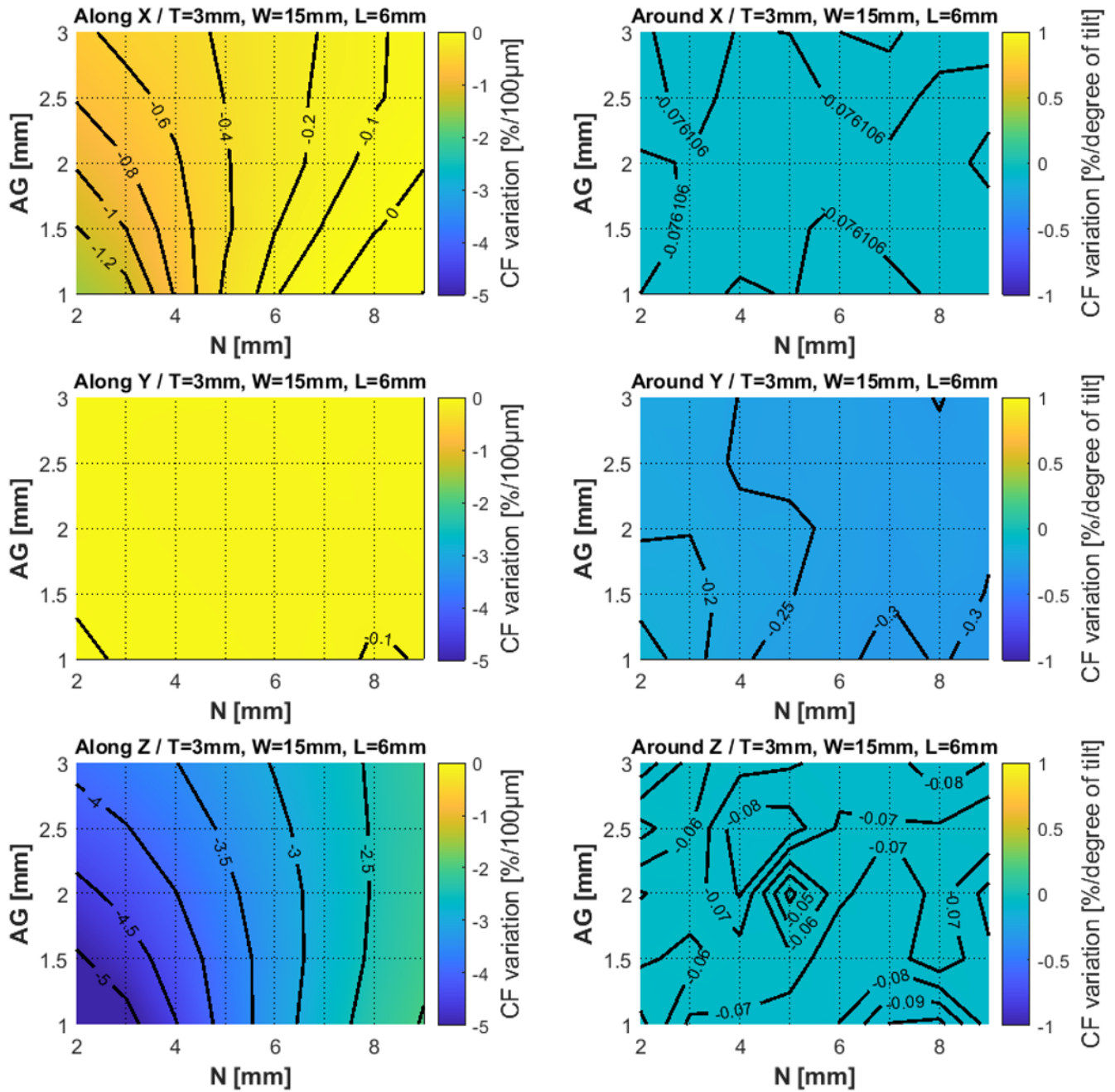


Figure 12: Coupling factor variations due to displacement along x, y, and z axis and rotation around x, y, and z (L = 6 mm, T = 3 mm, and W = 15 mm)

Choosing the Right Notch Dimensions

As already said, the key notch dimensions are its width N and its length L. Selecting the right dimensions results from a compromise between the application requirements.

As a summary:

- A narrow notch tends to improve the signal-to-noise ratio and the AC performances while it increases the additional heat, may weaken the busbar mechanical properties and increases the sensitivity to placement tolerances
- A long notch tends to improve the AC performances while it increases the additional heat and may weaken the busbar mechanical properties

There is no formal method to design the ideal notch dimensions as it highly depends on the application requirements and the mechanical and thermal constraints. However, a good starting point is N = 4 mm and L = 6 mm, which offers a good compromise between all the requirements and constraints. For DC application, one may want to reduce the length to L = 3 mm.

Selecting the Appropriate ACS37610 Part Number

Once the notch dimensions are chosen, the coupling factor is fixed. The required ACS37610 sensitivity is fixed as well, since it is directly linked to the coupling factor by equation 4. Then, from the application requirements (ΔI and ΔV) and the busbar dimensions, the procedure to select the appropriate ACS37610 part number is given in Figure 13. Thanks to the very wide range of the ACS37610 programming sensitivities, it will very likely cover most applications.

The most critical situation is at minimum air gap. The signal is maximum; therefore, the sensitivity range must be selected so that the output never saturates.

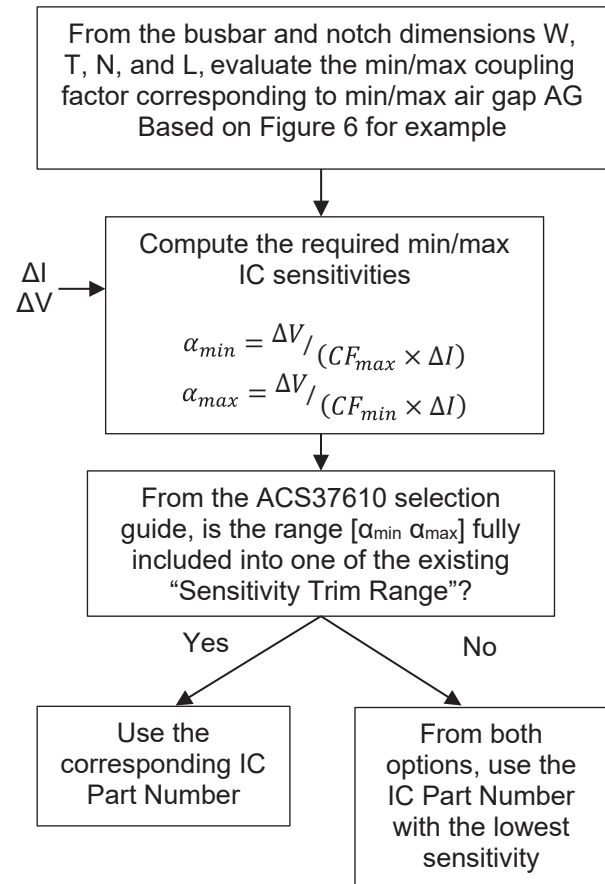


Figure 13: Procedure to select appropriate ACS37610 Part Number

Notch Design: An Example

What would be the optimum busbar design for an application example having:

- Current range: ± 1000 A
- Max current density 20 A/mm²
 - $W = 17$ mm
 - $T = 3$ mm
- $V_{CC} = 5$ V
- Air gap: 2.0 mm ± 0.5 mm
- Bandwidth: 50 kHz
- AC performances: phase shift $< 5^\circ$ at 2 kHz

Starting from $L = 6$ mm, Figure 10 tells us that the notch width must be $N = 4.5$ mm to achieve less than 5° of phase shift over the air gap range. From Figure 6, the coupling factor varies from 240 mG/A at maximum air gap to 380 mG/A at minimum air gap. Equation 4 and the procedure in Figure 13 indicate that the required ACS37610 sensitivity ranges from 5.2 to 8.4 mV/G ($\Delta V = 4000$ mV and $\Delta I = 2 \times 1000$ A); then the right part number is 10B5.

The corresponding performances are:

- Current noise: 0.95 A_{rms} (Figure 7)
- Effective resolution: 8.5 bits (based on the 6-sigma noise)
- Gain: -3% @ 2 kHz (Figure 9)
- Additional resistance: 8.5 $\mu\Omega$ (from previous section): equivalent to 4.25 W

Conclusions

The notch must be designed carefully to accommodate for the application DC and AC requirements and for mechanical and thermal constraints.

This application note offers guidelines for achieving the optimum notch design using the Allegro ACS37610 coreless current sensor. When well-designed, current ranges from two hundred ampere to some thousands of amperes can be measured with high accuracy and high resolution.

Contact an Allegro representative for any further questions or support.

Appendix

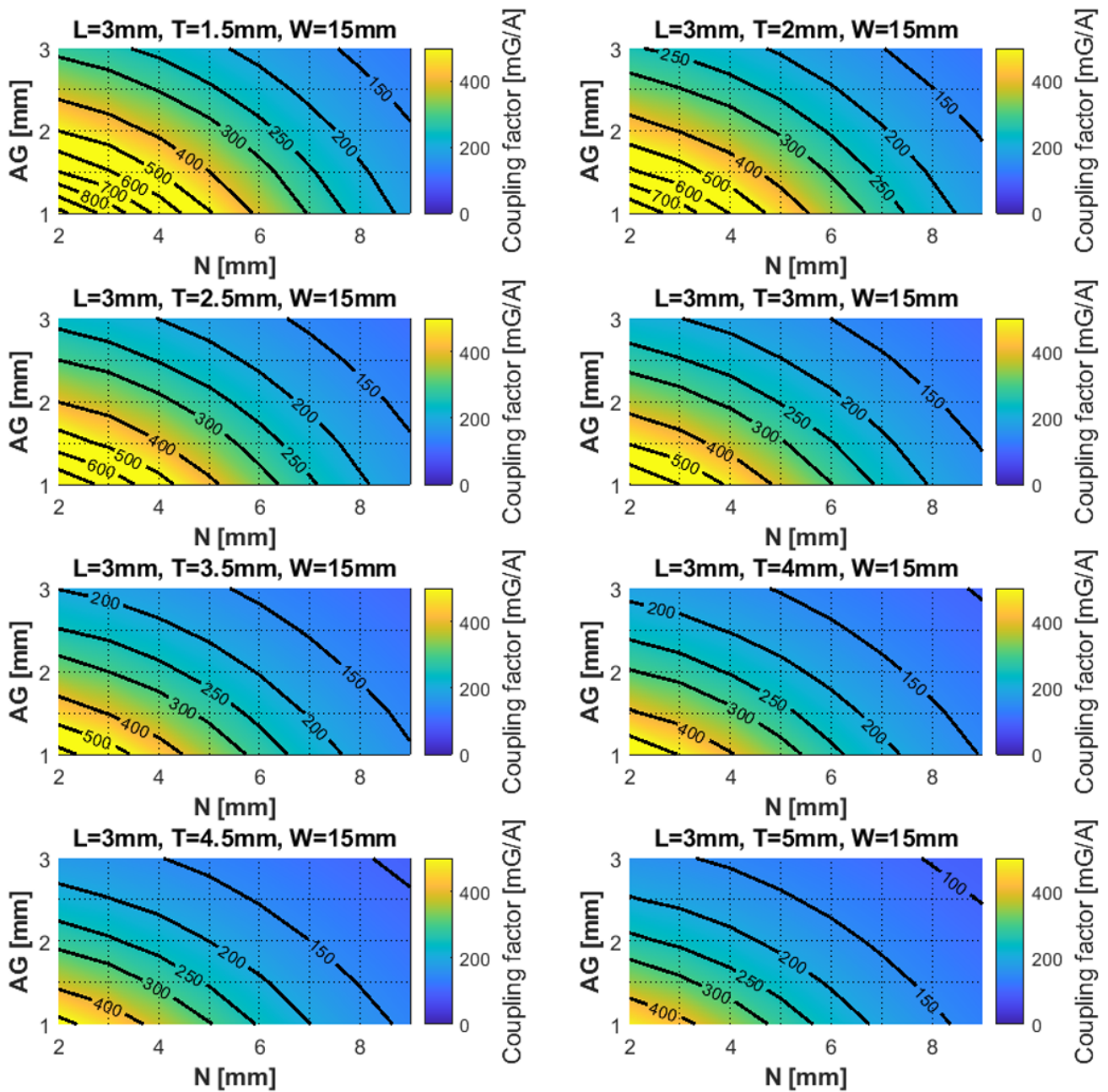


Figure 14: Coupling factor versus AG and N for various busbar thicknesses (L = 3 mm, W = 15 mm)

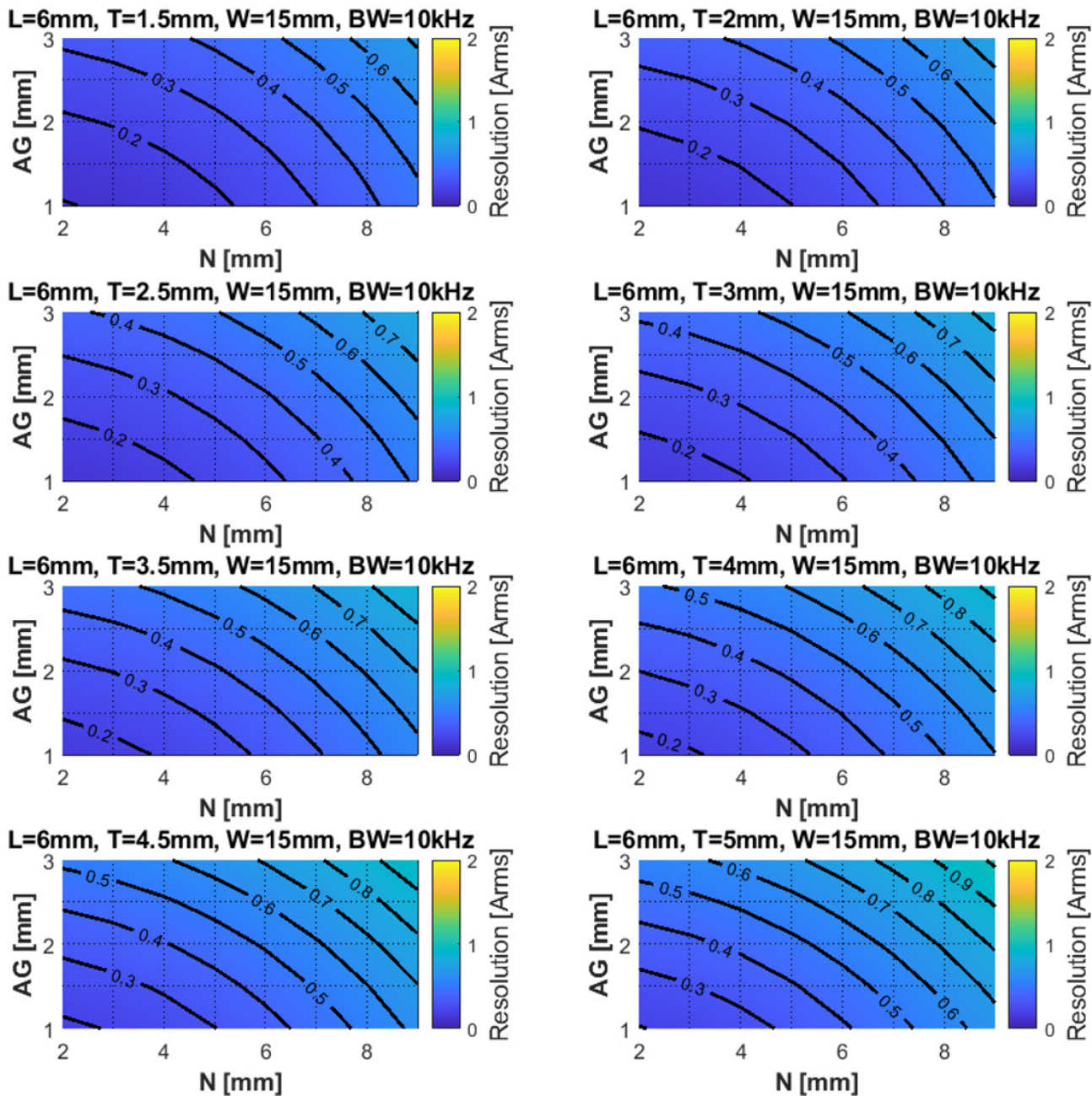


Figure 15: Resolution versus AG and N for various busbar thicknesses, at 10 kHz ($L = 6\text{ mm}$, $W = 15\text{ mm}$)

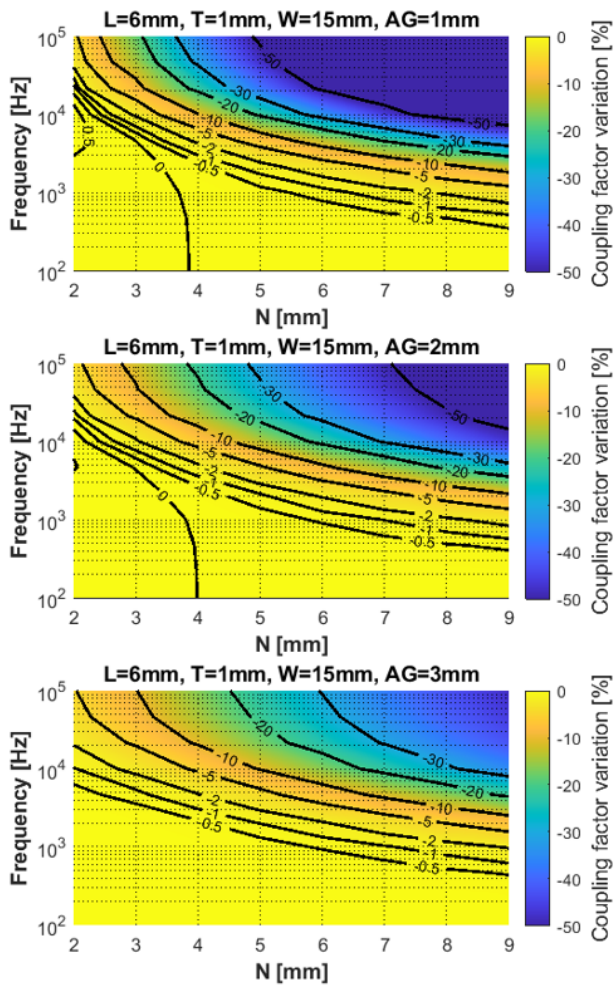


Figure 16: Coupling factor loss over frequency and air gap, due to eddy current in the busbar ($L = 6 \text{ mm}$, $T = 1 \text{ mm}$, $W = 15 \text{ mm}$)

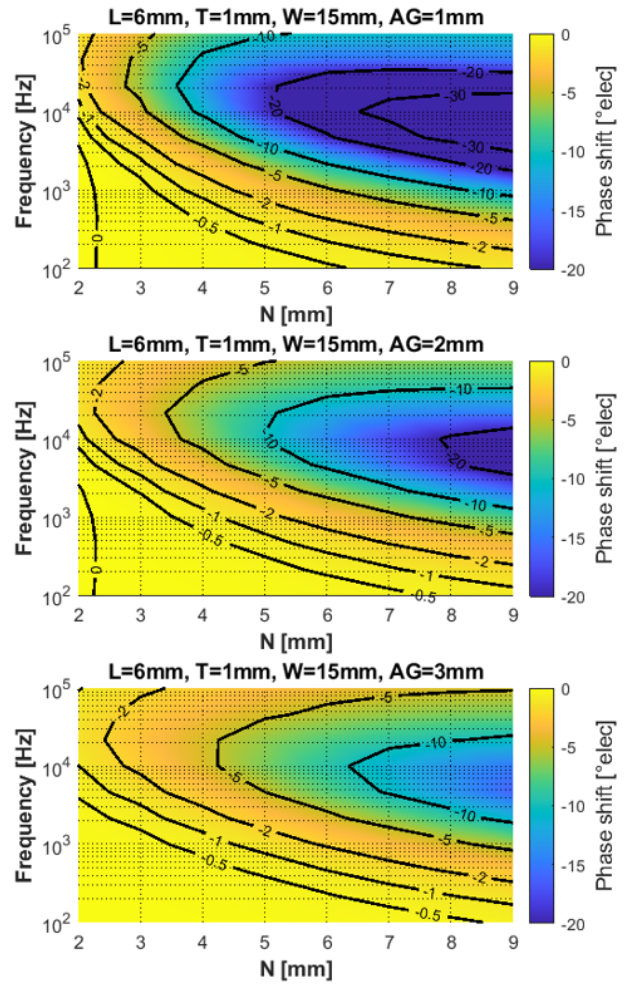


Figure 17: Phase delay over frequency and air gap, due to eddy current in the busbar ($L = 6 \text{ mm}$, $T = 1 \text{ mm}$, $W = 15 \text{ mm}$)

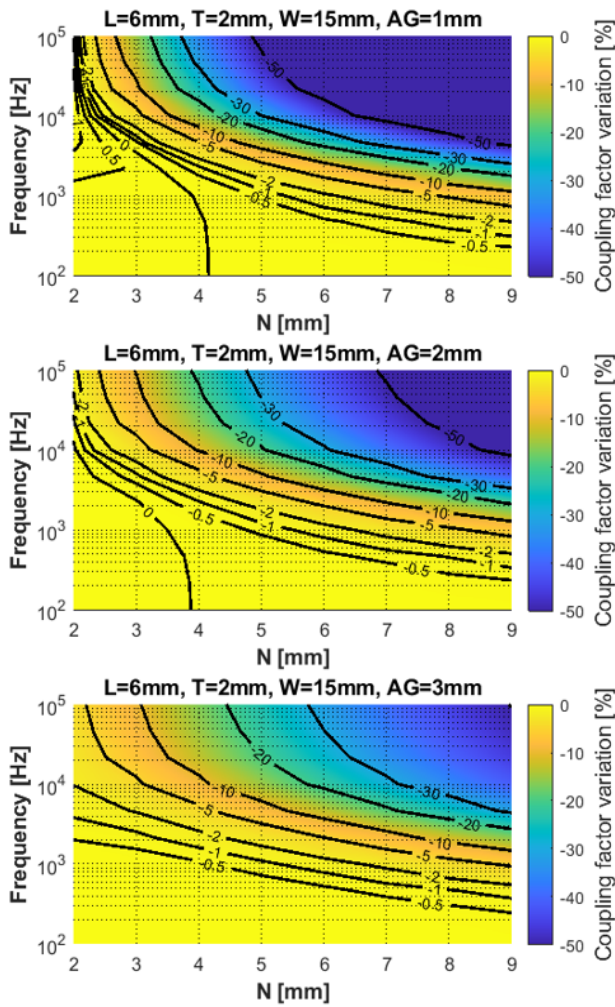


Figure 18: Coupling factor loss over frequency and air gap, due to eddy current in the busbar (L = 6 mm, T = 2 mm, W = 15 mm)

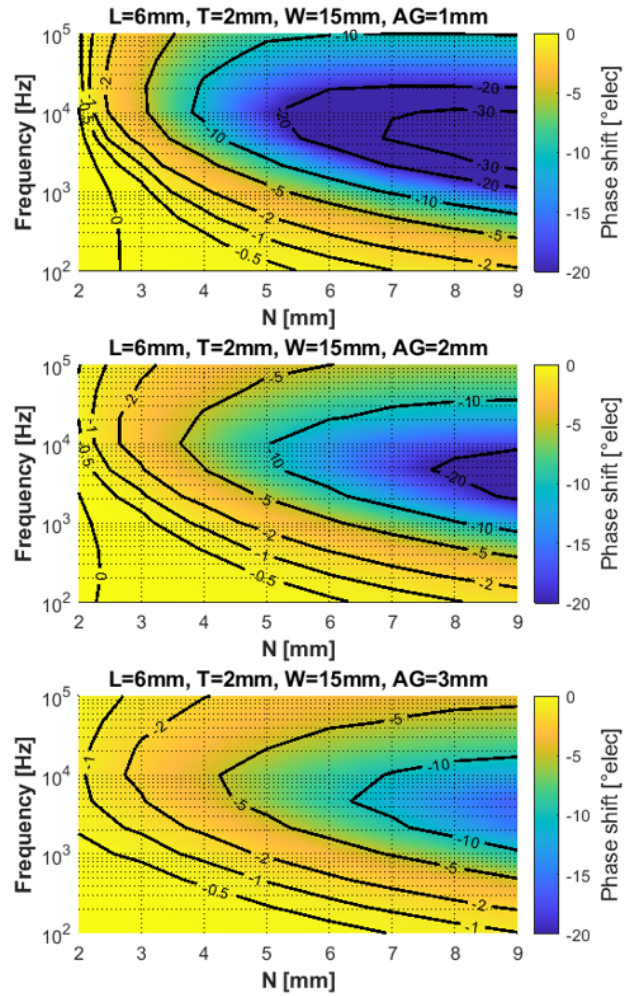


Figure 19: Phase delay over frequency and air gap, due to eddy current in the busbar (L = 6 mm, T = 2 mm, W = 15 mm)

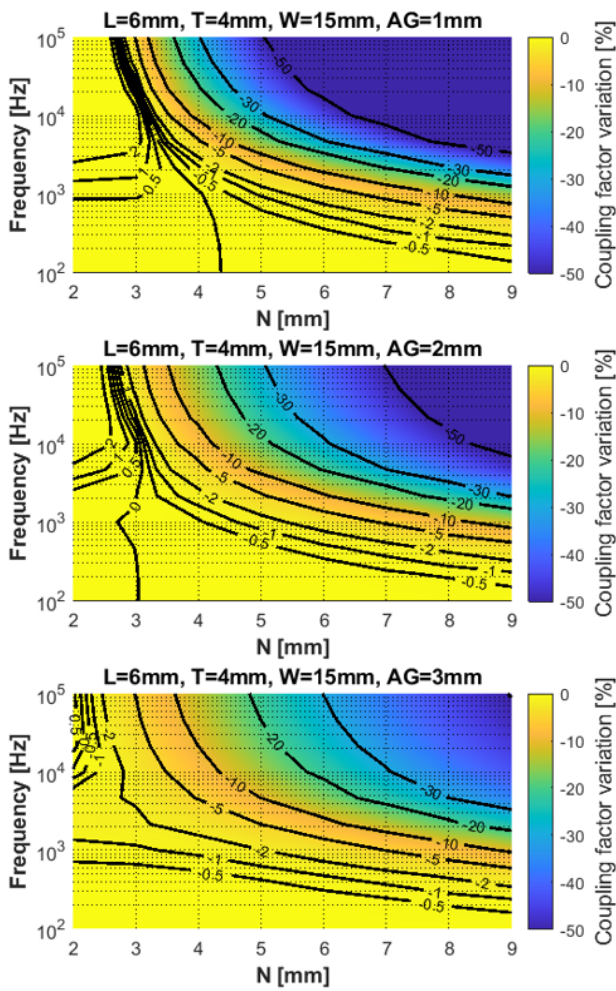


Figure 20: Coupling factor loss over frequency and air gap, due to eddy current in the busbar (L = 6 mm, T = 4 mm, W = 15 mm)

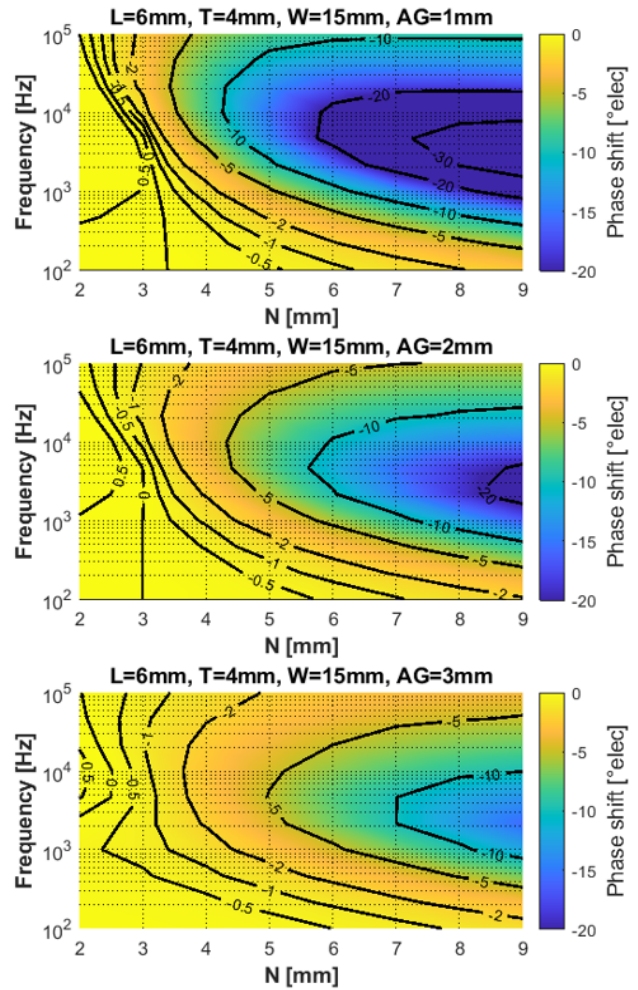


Figure 21: Phase delay over frequency and air gap, due to eddy current in the busbar (L = 6 mm, T = 4 mm, W = 15 mm)

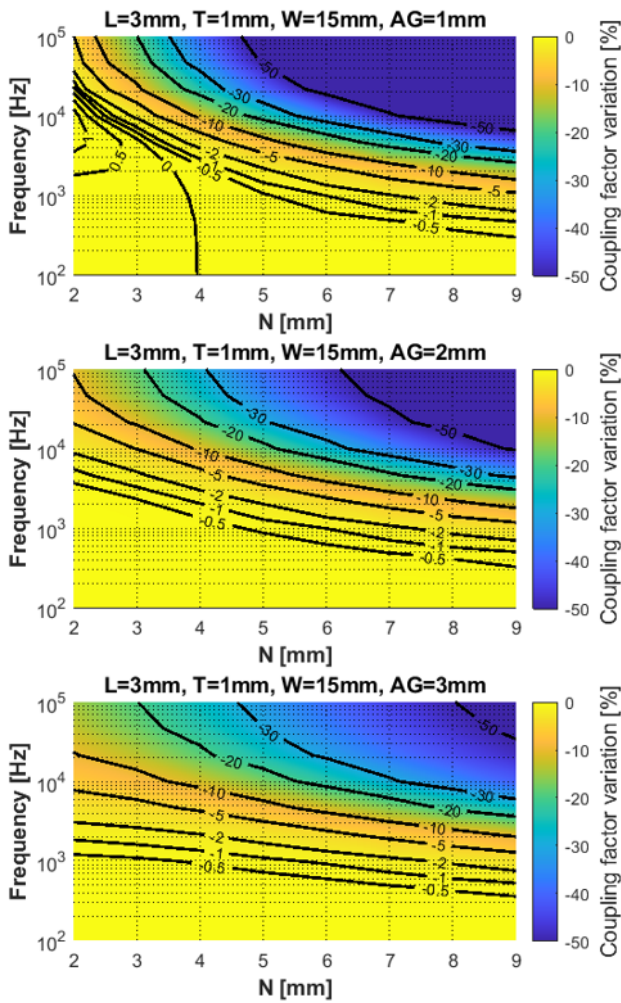


Figure 22: Coupling factor loss over frequency and air gap, due to eddy current in the busbar ($L = 3 \text{ mm}$, $T = 1 \text{ mm}$, $W = 15 \text{ mm}$)

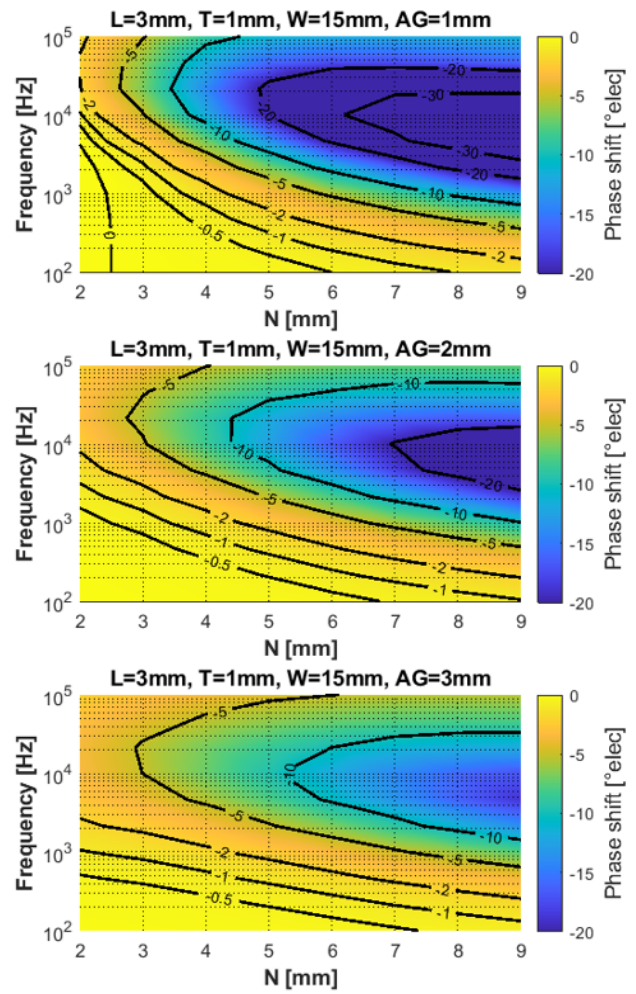


Figure 23: Phase delay over frequency and air gap, due to eddy current in the busbar ($L = 3 \text{ mm}$, $T = 1 \text{ mm}$, $W = 15 \text{ mm}$)

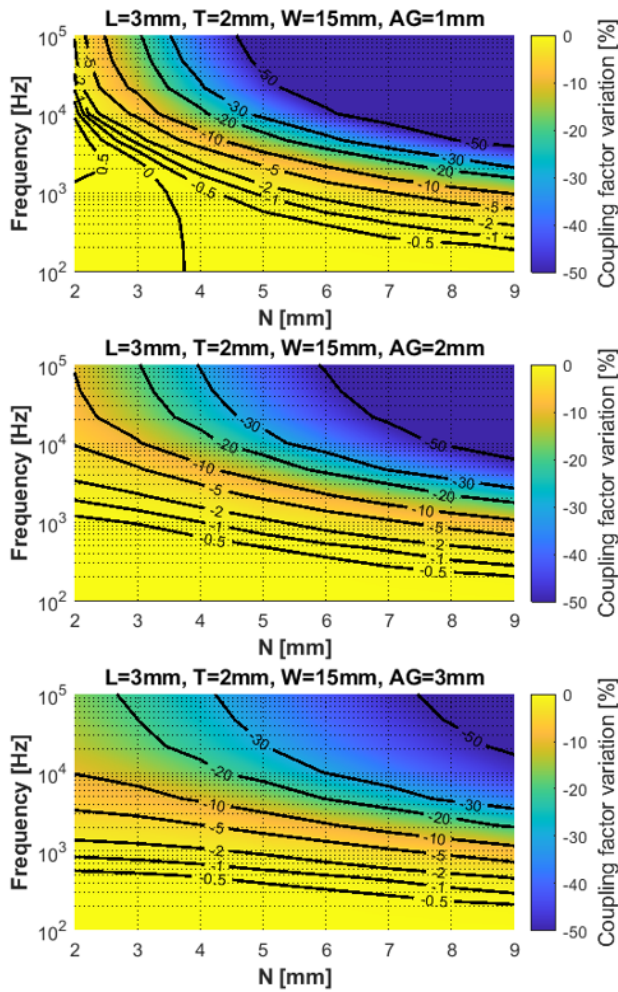


Figure 24: Coupling factor loss over frequency and air gap, due to eddy current in the busbar ($L = 3 \text{ mm}$, $T = 2 \text{ mm}$, $W = 15 \text{ mm}$)

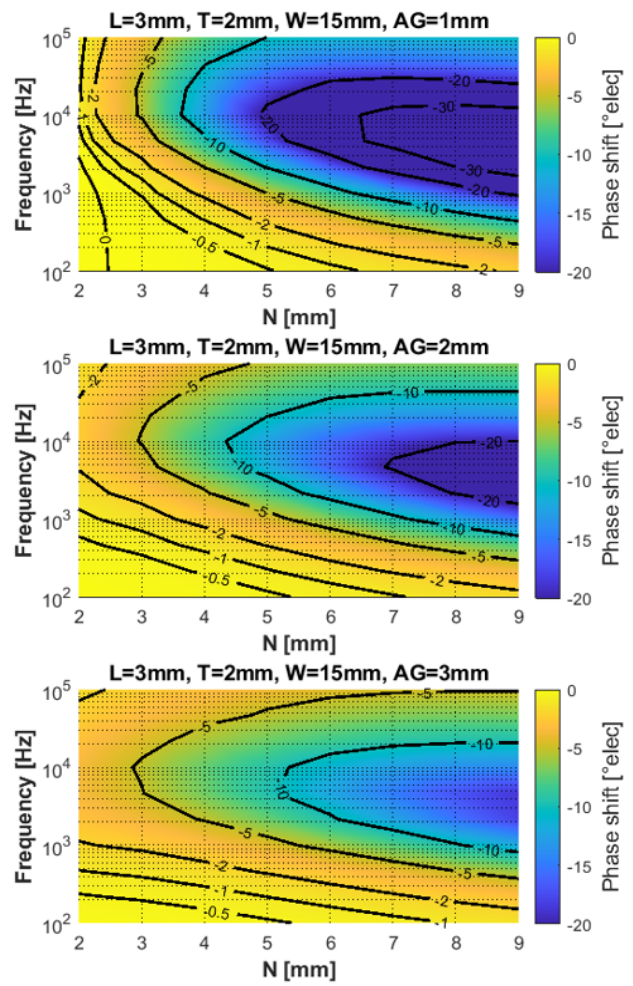


Figure 25: Phase delay over frequency and air gap, due to eddy current in the busbar ($L = 3 \text{ mm}$, $T = 2 \text{ mm}$, $W = 15 \text{ mm}$)

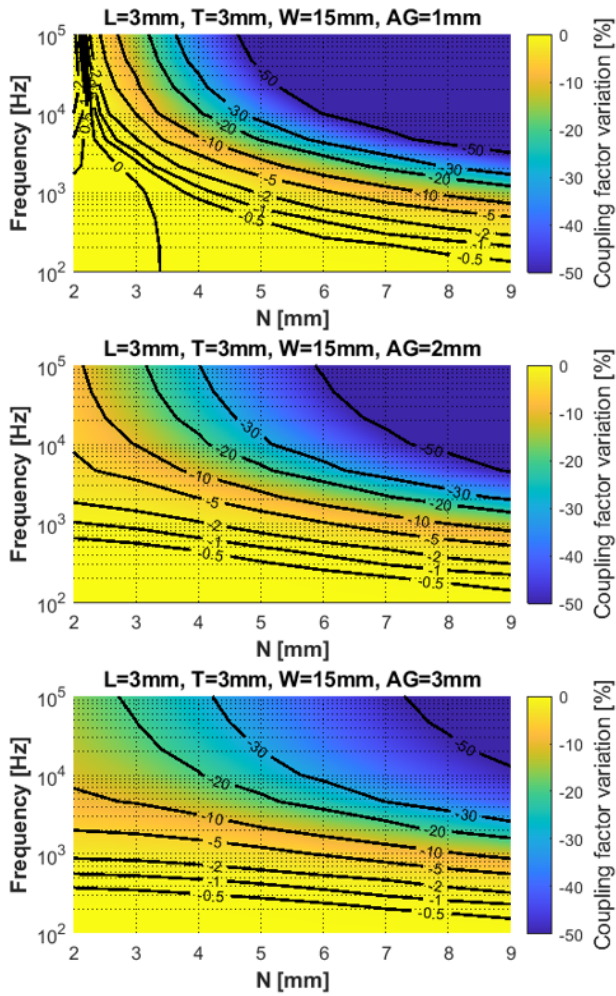


Figure 26: Coupling factor loss over frequency and air gap, due to eddy current in the busbar ($L = 3 \text{ mm}$, $T = 3 \text{ mm}$, $W = 15 \text{ mm}$)

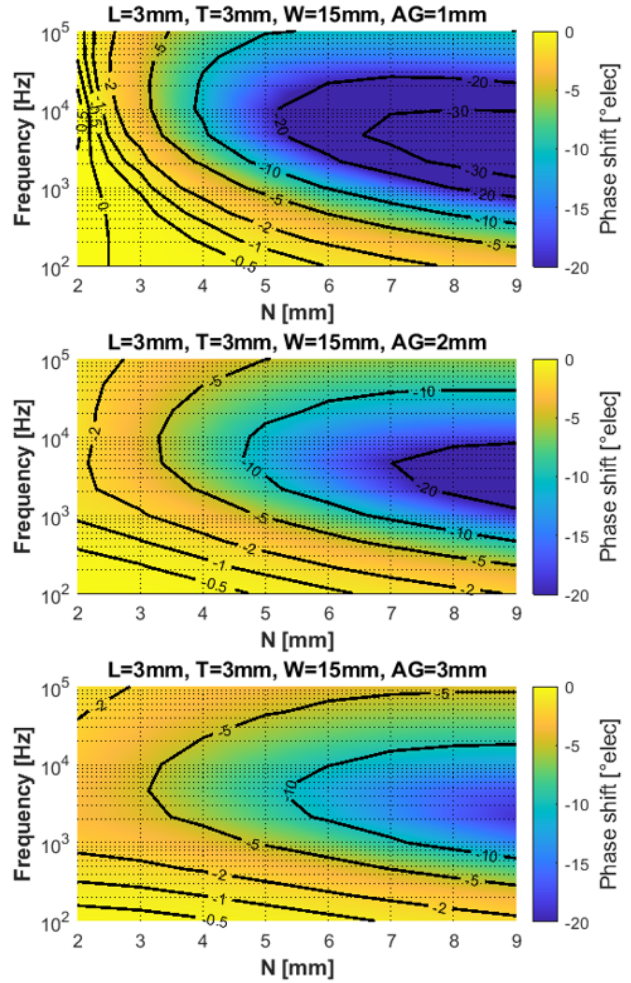


Figure 27: Phase delay over frequency and air gap, due to eddy current in the busbar ($L = 3 \text{ mm}$, $T = 3 \text{ mm}$, $W = 15 \text{ mm}$)

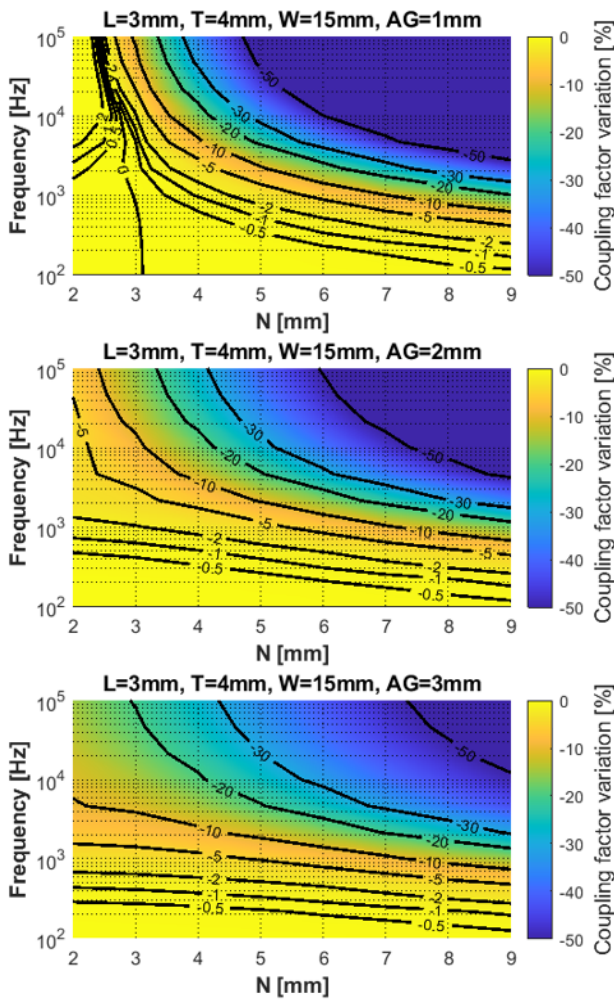


Figure 28: Coupling factor loss over frequency and air gap, due to eddy current in the busbar (L = 3 mm, T = 4 mm, W = 15 mm)

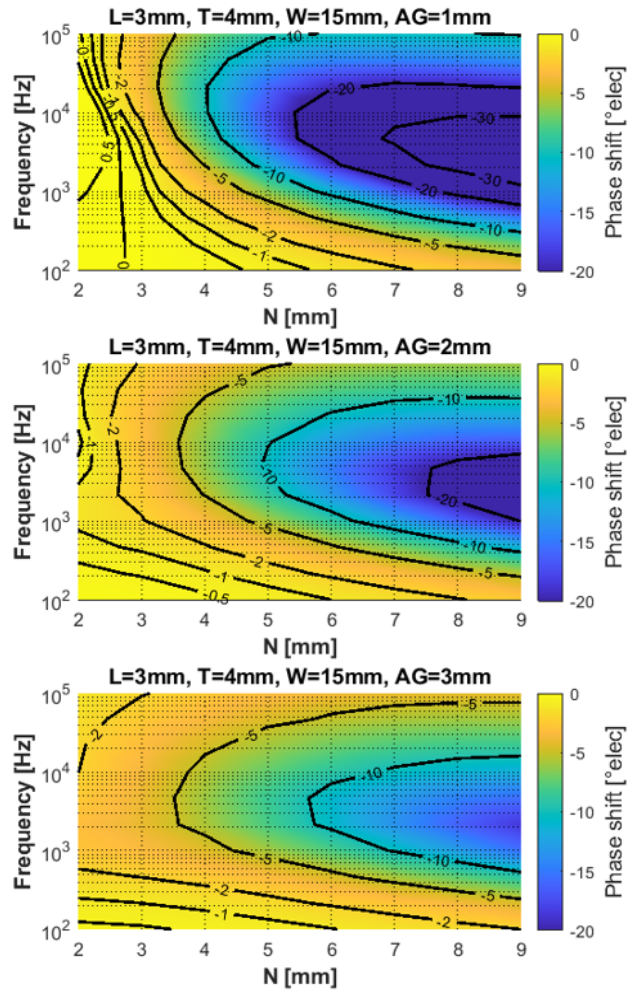


Figure 29: Phase delay over frequency and air gap, due to eddy current in the busbar (L = 3 mm, T = 4 mm, W = 15 mm)

Revision History

Number	Date	Description	Responsibility
-	February 22, 2021	Initial release	Y. Vuillermet
1	October 26, 2021	Updated figure 2.	Y. Vuillermet

Copyright 2021, Allegro MicroSystems.

The information contained in this document does not constitute any representation, warranty, assurance, guaranty, or inducement by Allegro to the customer with respect to the subject matter of this document. The information being provided does not guarantee that a process based on this information will be reliable, or that Allegro has explored all of the possible failure modes. It is the customer's responsibility to do sufficient qualification testing of the final product to ensure that it is reliable and meets all design requirements.

Copies of this document are considered uncontrolled documents.